

Linking electronic and molecular structure: Insight into aqueous chloride solvation

Ling Ge^{*†}, Leonardo Bernasconi[‡], and Patricia Hunt[†]

[†]Department of Chemistry, Imperial College London, London SW7 2AZ,
United Kingdom

[‡]STFC Rutherford Appleton Laboratory, Didcot, Oxfordshire OX11 0QX,
United Kingdom

Supplementary Information

Brief Discussion of the EMO Method.

The EMO method interprets the time evolution of the electronic and molecular structure of both solute and solvent. Briefly, the EMO method for analysing the electronic structure of solutes and solvents starts by considering the Kohn-Sham Hamiltonian and energy eigenvalues obtained from the *ab-initio* MD. Orbitals obtained by diagonalising the Kohn-Sham Hamiltonian in an extended system have a Bloch form, and are therefore delocalised over the whole space. In a molecular liquid, the Kohn-Sham orbital energies are well-defined, however, they do not necessarily yield information about the local electronic structure of individual solvent molecules, **Figure S1(a)**. This makes it difficult to analyse interactions between an ion and the solvating solvent molecules. Maximally localised Wannier orbitals are local to atomic (or bond) centers. However, the Hamiltonian in the Wannier basis is no longer diagonal, and thus there is no unique energy eigenvalue that can be associated with each orbital, **Figure S1(c)**. An intermediate representation where orbitals are local to a molecule, but are delocalised within the molecule has been developed. The EMOs are obtained by assigning Wannier orbitals to a specific molecule, and block-diagonalising the Wannier Hamiltonian within the molecular subspace, **Figure S1(b)**.

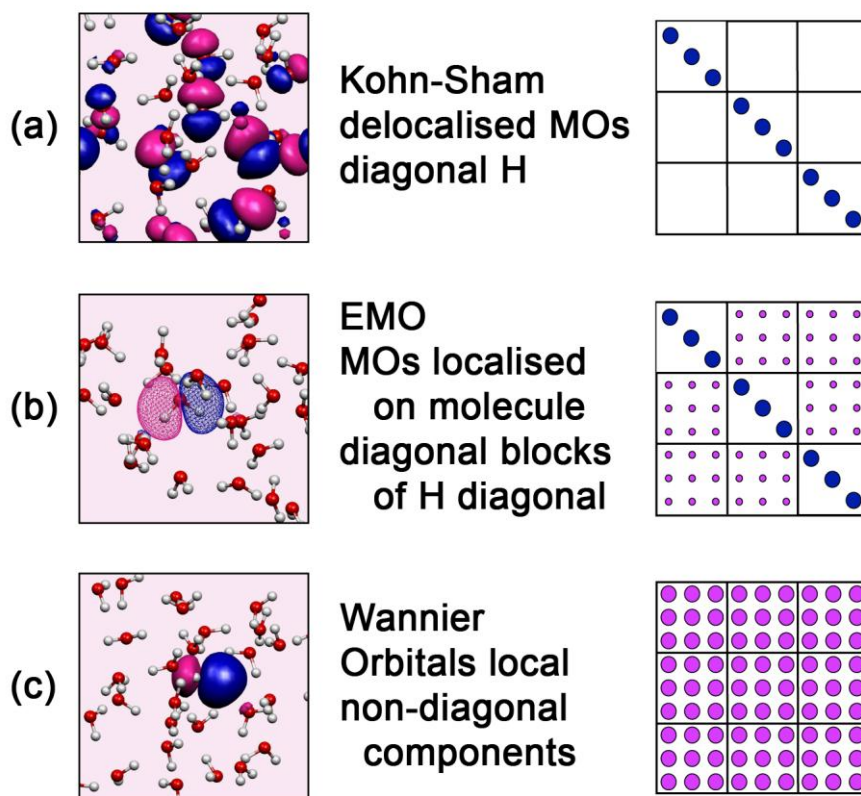


Figure S1: Schematic representation of the structure of the DFT Hamiltonian in the (a) Kohn-Sham, (b) EMO and (c) Wannier representation for a pure liquid water atomic configuration obtained from a CPMD simulation at 298 K.

Each Wannier orbital is unambiguously associated with an atom and hence with a particular molecule. The EMOs are obtained by diagonalising blocks of the Wannier Hamiltonian within each molecular subspace and represent the electronic structure of individual solute and solvent molecules within the liquid. Each element of the EMO Hamiltonian matrix contributes either to a diagonal molecular block or to an off-diagonal intermolecular block, **Figure S2**. In a diagonal block all the Wannier orbitals are located on the same molecule and after diagonalisation these elements are interpreted as the effective “energy” of the EMOs (α_{xi}). After diagonalisation small but finite elements remain in the off-diagonal blocks, representing electronic coupling ($\beta_{xi,yj}$) between the two molecules, where $x \neq y$ are molecule indices and i, j are orbital indices.

	molecule 1	molecule 2	etc
molecule 1	α_{1i} 0	$\beta_{1i,2i}$ $\beta_{1i,2j}$	
	0 α_{1j}	$\beta_{1j,2i}$ $\beta_{1j,2j}$	
molecule 2	$\beta_{2i,1i}$ $\beta_{2i,1j}$	α_{2i} 0	
	$\beta_{2j,1i}$ $\beta_{2j,1j}$	0 α_{2j}	
etc			

Figure S2: Representation of the EMO Hamiltonian matrix.

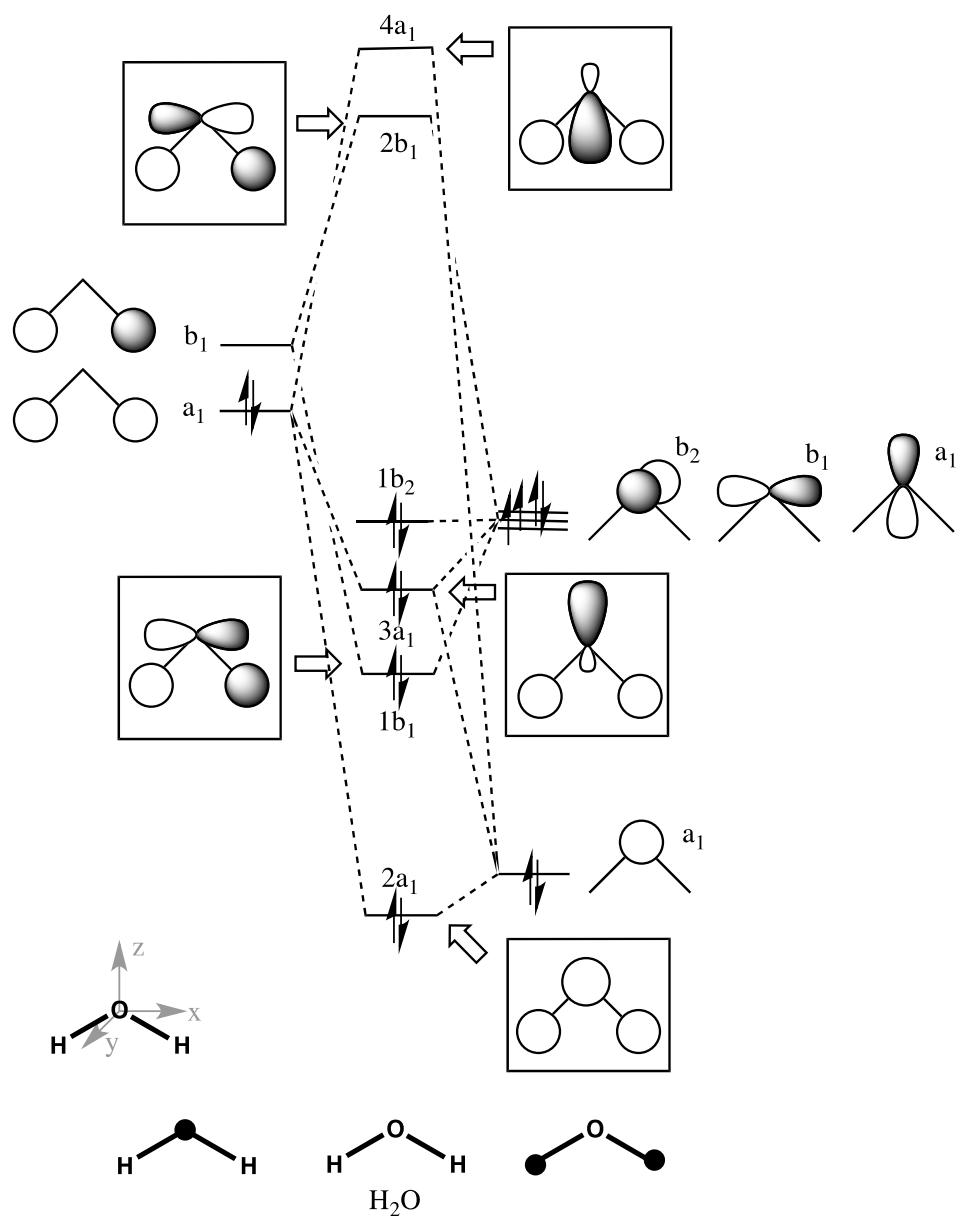


Figure S3: Molecular orbital diagram for an isolated water molecular with C_{2v} symmetry.

The EMO approach is sufficiently general to be used on gas-phase systems, as well as condensed (periodic) systems. **Figure S4** is an illustrative example of the application of the EMO method to a simple gas-phase ($\text{Cl}^- + \text{H}_2\text{O}$) cluster.

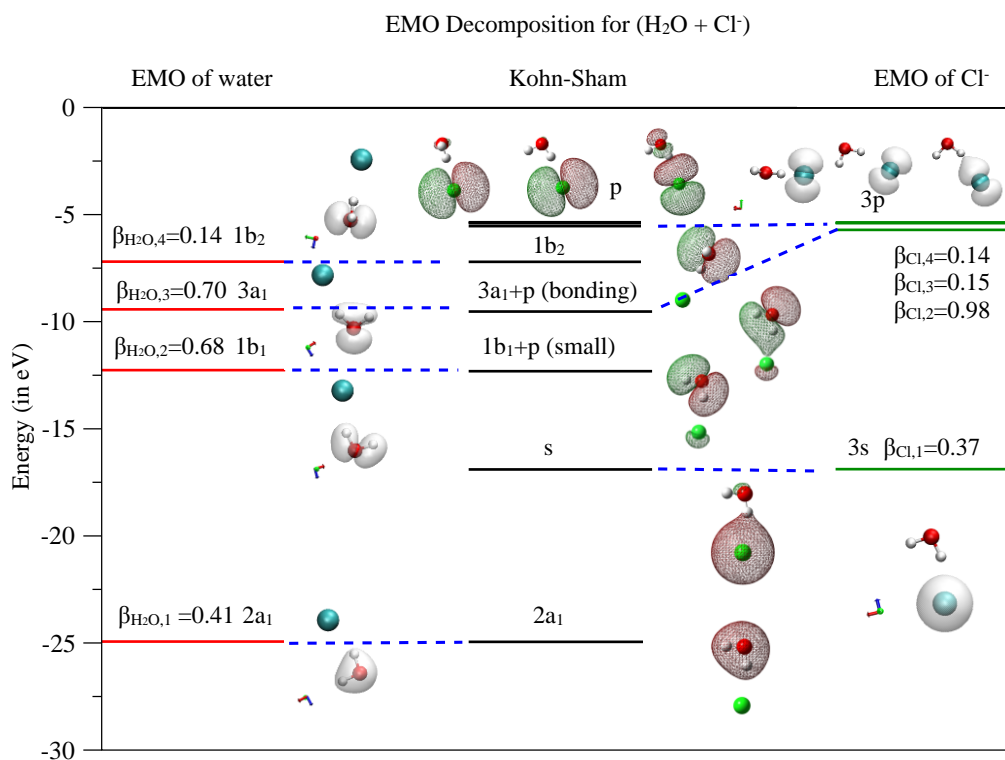


Figure S4: EMO decomposition of the Kohn-Sham MOs of ($\text{H}_2\text{O} + \text{Cl}^-$) in gas phase. The middle panel shows the Kohn-Sham energy levels and MOs. The left and right panels show the Cl^- and H_2O effective energy levels and MOs, respectively, which resemble those of a Cl^- and H_2O in the gas phase.

Table S1. EMO beta parameters derived from the PBE calculations (on the three selected structures identified in the text). BLYP and PBE give almost identical results (BLYP results presented in Table 3 of the paper).

	low Cl ⁻	level Cl ⁻	high Cl ⁻
PBE	HOMO	HOMO	HOMO
	5(c)	5(b)	5(a)
$\beta_{1stshell-Cl}$	0.178	0.205	0.136
$\beta_{bulk-Cl}$	0.003	0.004	0.004
$\beta_{1stshell-bulk}$	0.014	0.014	0.013
β_{bulk}	0.017	0.017	0.017

Table 3 EMO β parameters for the structures shown in 5.

	low Cl ⁻	level Cl ⁻	high Cl ⁻
	HOMO	water HOMOs	HOMO
	5(c)	5(b)	5(a)
$\beta_{1stshell-Cl}$	0.179	0.206	0.137
$\beta_{bulk-Cl}$	0.004	0.004	0.004
$\beta_{1stshell-bulk}$	0.014	0.014	0.013
β_{bulk}	0.017	0.017	0.018

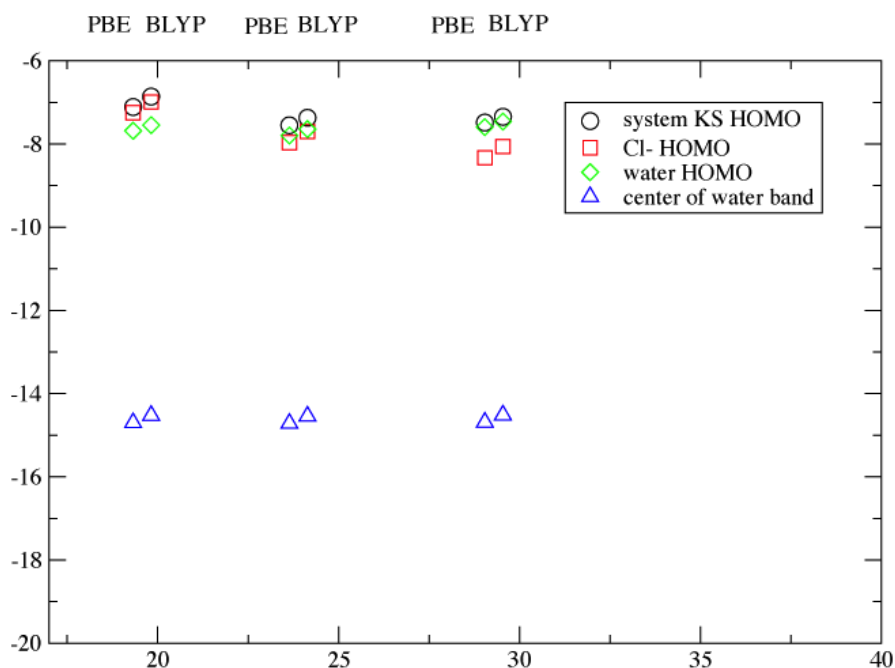


Figure S5: EMO orbital energies compared for BLYP and PBE. Calculations carried out on the three selected snapshots identified in the main text of the paper. BLYP and PBE give almost identical results.

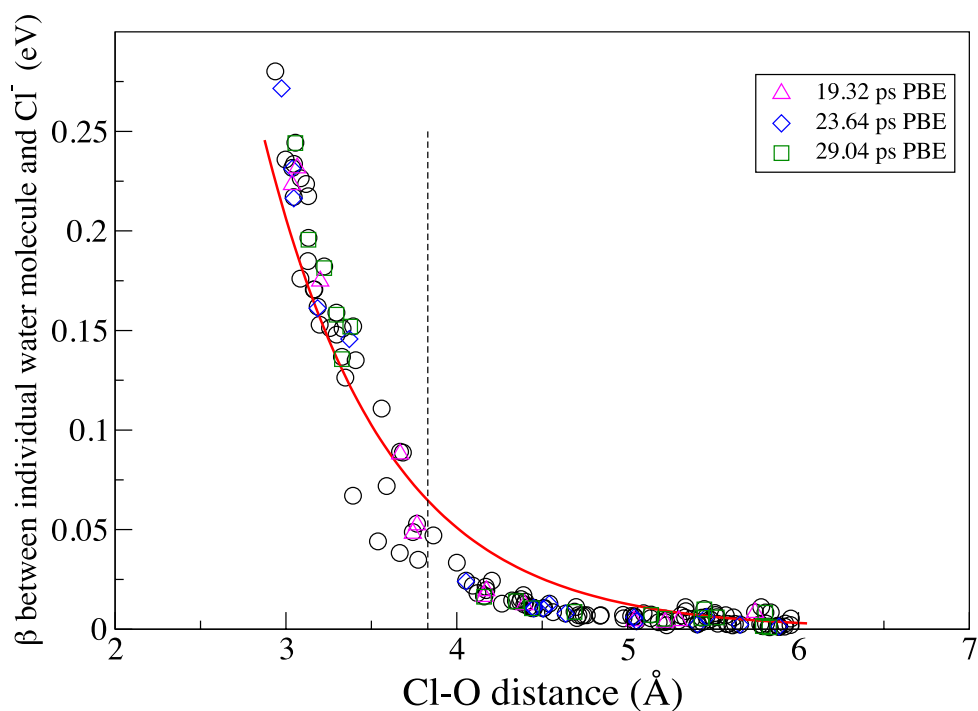


Figure S6: β as a function of Cl-O distance, the circles are the BLYP results reported in **Figure 7** from the main text, the PBE data are the open triangles, diamonds and squares as identified in the legend. The PBE results are almost identical to the BLYP results.

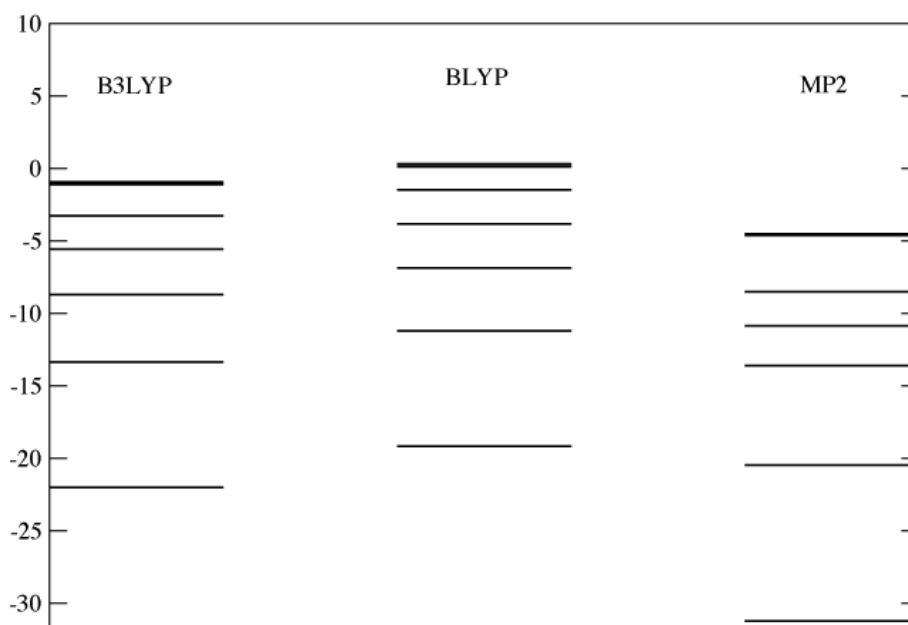


Figure S7: Electronic structure of gas phase $\text{H}_2\text{O} + \text{Cl}^-$ (B3LYP/BLYP/MP2) BLYP and B3LYP underestimate the gap between the 3-fold degenerate HOMO level (Cl HOMO) and HOMO-1 (water HOMO).

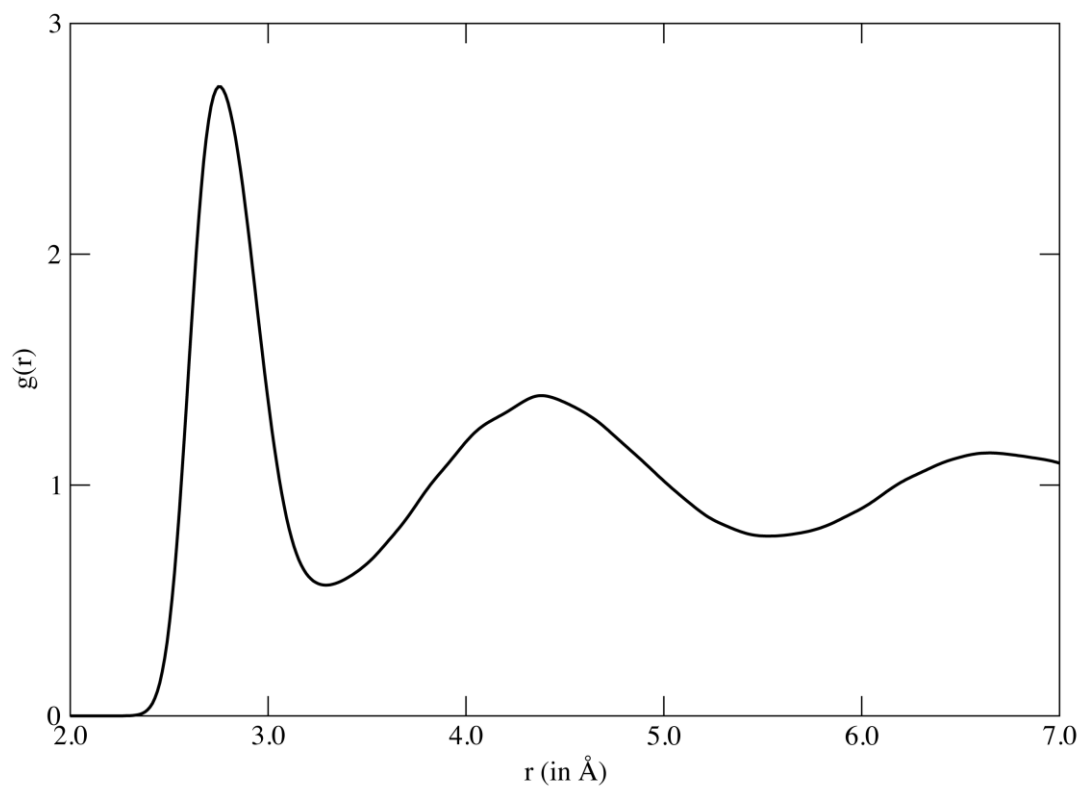


Figure S8: O-O radial distribution function.

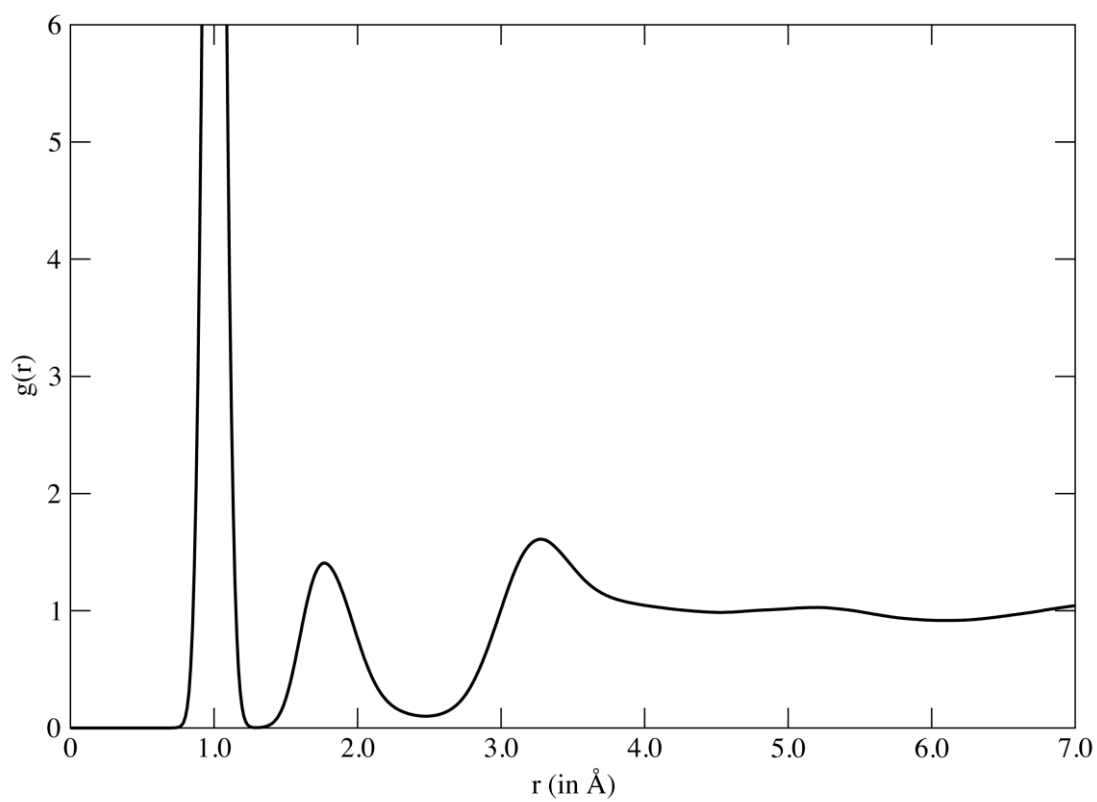


Figure S9: O-H radial distribution function.

Table S2: Kohn-Sham HOMO Energy (eV) and EMO α parameters for the structures shown in **Figure 5** of the main article.

	low Cl ⁻ HOMO 5(c)	level Cl ⁻ water HOMOs 5(b)	high Cl ⁻ HOMO 5(a)
System KS HOMO	-9.66	-9.68	-9.17
Cl ⁻ HOMO, α_{Cl}	-10.37	-10.01	-9.30
water HOMO, α_{H_2O}	-9.77	-9.95	-9.86
first solvation shell water HOMOs	-11.43 -11.04 -10.68 -10.63 -10.60 -10.39	-11.62 -11.31 -10.86 -10.60 -10.52 -	-10.99 -10.76 -10.73 -10.69 -10.45 -10.35

Table S3: EMO β parameters for the water molecules within the first solvation shell of the structures shown in **Figure 5** of the main article.

low Cl ⁻ HOMO 5(c)		level Cl ⁻ water HOMOs 5(b)		high Cl ⁻ HOMO 5(a)	
type	<i>beta</i>	type	<i>beta</i>	type	<i>beta</i>
H-bonding	0.182	H-bonding	0.217	H-bonding	0.175
H-bonding	0.244	H-bonding	0.146	H-bonding	0.232
H-bonding	0.197	H-bonding	0.162	H-bonding	0.224
H-bonding	0.153	H-bonding	0.272	H-bonding	0.089
H-bonding	0.137	H-bonding	0.232	local	0.053
H-bonding	0.159	-	-	local	0.048
total	1.072	total	1.029	total	0.822

Table S4: Association energies ΔE for $(\text{H}_2\text{O})_2$ and $(\text{H}_2\text{O} + \text{Cl}^-)$

System	ΔE_{opt} (kJ/mol)	ΔE_{ZPE} (kJ/mol)	ΔE_{BSSE} (kJ/mol)	ΔE (kJ/mol)
$(\text{H}_2\text{O})_2$	-31.5	13.9	8.0	-9.6
$\text{H}_2\text{O} + \text{Cl}^-$	-74.6	7.9	10.7	-56.0

Table S5: Conformer energies of the MP2/cc-pVTZ optimized structures of the $[\text{Cl}(\text{H}_2\text{O})_5]^-$ and $[\text{Cl}(\text{H}_2\text{O})_6]^-$ clusters. oop=out-of-plane, ip=in-plane

System	Final coordination	ΔE_{MP2} (kJ/mol)	$\Delta E_{\text{MP2+ZPE}}$ (kJ/mol)	ΔG_{MP2} (kJ/mol)
$[\text{Cl}(\text{H}_2\text{O})_5]^-$	4 H-bonding	5.4	2.6	4.3
	5 H-bonding	0.0	0.0	0.0
$[\text{Cl}(\text{H}_2\text{O})_6]^-$	6 H-bonding	15.9	11.1	0.0
	4 H-bonding (oop)	0.0	0.0	4.0
	4 H-bonding (ip)	21.3	17.2	14.9
	3 H-bonding	14.4	11.1	9.2

Table S6: Conformer energies of the B3LYP/cc-pVTZ optimized structures of the $[\text{Cl}(\text{H}_2\text{O})_5]^-$ and $[\text{Cl}(\text{H}_2\text{O})_6]^-$ clusters. oop=out-of-plane, ip=in-plane

System	Final coordination	ΔE_{B3LYP} (kJ/mol)	$\Delta E_{\text{B3LYP+ZPE}}$ (kJ/mol)	ΔG_{B3LYP} (kJ/mol)
$[\text{Cl}(\text{H}_2\text{O})_5]^-$	4 H-bonding	3.6	2.5	0.0
	5 H-bonding	0.0	0.0	15.3
$[\text{Cl}(\text{H}_2\text{O})_6]^-$	6 H-bonding	13.3	9.7	0.0
	4 H-bonding (oop)	0.0	0.0	5.6
	3 H-bonding (ip)	14.5	10.6	8.4
	3 H-bonding (oop)	4.6	2.0	4.4

Table S7: HOMO and LUMO levels of the MP2/cc-pVTZ optimized structures of the $[\text{Cl}(\text{H}_2\text{O})_5]^-$ and $[\text{Cl}(\text{H}_2\text{O})_6]^-$ clusters, VBE is the valence band edge of the water component. oop=out-of-plane, ip=in-plane

System	Final coordination	water VBE (eV)	HOMO (eV)	LUMO (eV)	ΔE homo-lumo gap (eV)	ΔE VBE-homo gap (eV)
$[\text{Cl}(\text{H}_2\text{O})_5]^-$	4 H-bonding	-9.18	-6.90	7.22	14.12	2.28
	5 H-bonding	-9.76	-6.81	8.00	14.81	2.95
$[\text{Cl}(\text{H}_2\text{O})_6]^-$	6 H-bonding	-10.05	-7.55	7.71	15.26	2.50
	4 H-bonding (oop)	-9.76	-7.04	7.59	14.63	2.72
	4 H-bonding (ip)	-9.83	-6.98	7.03	14.01	2.85
	3 H-bonding	-9.63	-6.61	7.26	13.87	3.02

Table S8: HOMO and LUMO levels of the B3LYP/cc-pVTZ optimized structures of the $[\text{Cl}(\text{H}_2\text{O})_5]^-$ and $[\text{Cl}(\text{H}_2\text{O})_6]^-$ clusters, VBE is the valence band edge of the water component.

System	Final coordination	water VBE (eV)	HOMO (eV)	LUMO (eV)	ΔE homo-lumo gap (eV)	ΔE VBE-homo gap (eV)
$[\text{Cl}(\text{H}_2\text{O})_5]^-$	4 H-bonding	-4.00	-3.29	3.94	7.33	0.71
	5 H-bonding	-4.66	-3.00	4.45	7.45	1.66
$[\text{Cl}(\text{H}_2\text{O})_6]^-$	6 H-bonding	-5.00	-3.89	4.08	7.97	1.11
	4 H-bonding (oop)	-4.75	-3.40	3.97	7.37	1.35
	3 H-bonding (ip)	-4.52	-3.20	3.81	7.01	1.32
	3 H-bonding (oop)	-4.64	-3.03	3.96	6.99	1.61

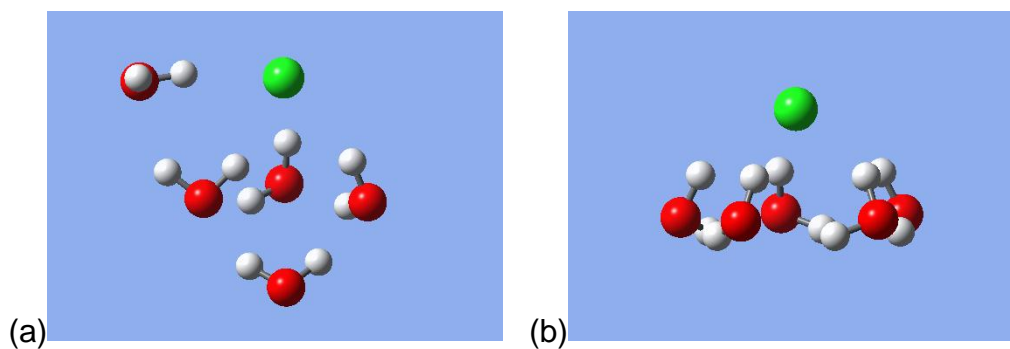


Figure S10: $[\text{Cl}(\text{H}_2\text{O})_5]^-$ (a) 4 H-bonding and 1 local water molecule and (b) 5 H-bonding and no local water molecules

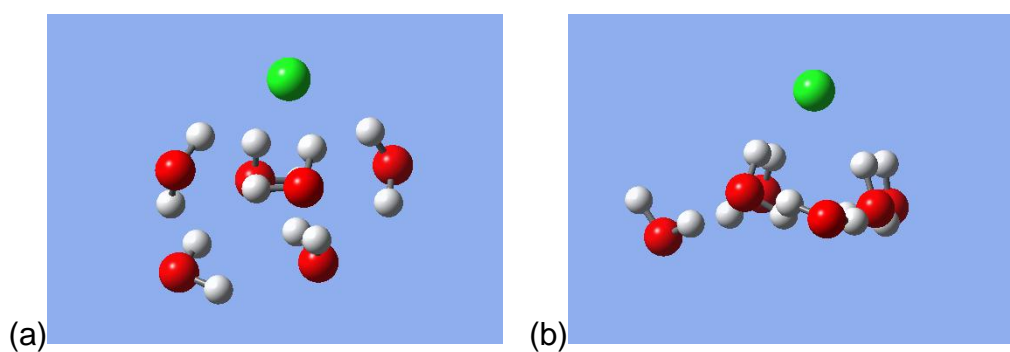


Figure S11: $[\text{Cl}(\text{H}_2\text{O})_6]^-$ two configurations with 4 H-bonding and two local water molecules

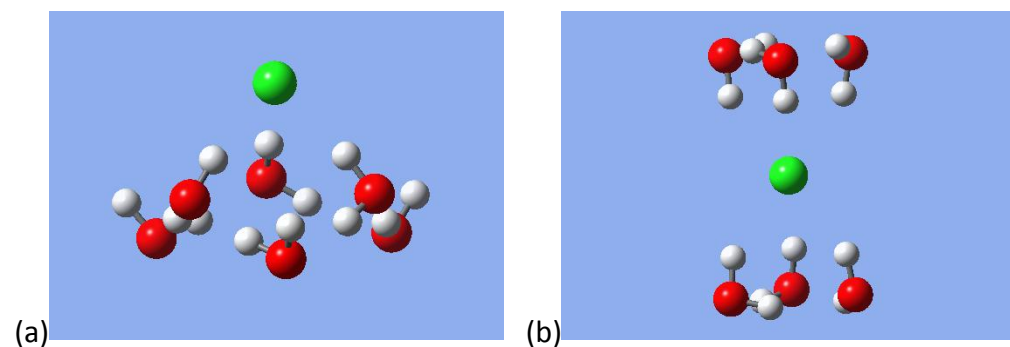


Figure S12: $[\text{Cl}(\text{H}_2\text{O})_6]^-$ (a) 3 H-bonding and 3 local water molecules and (b) 6 H-bonding and no local water molecules

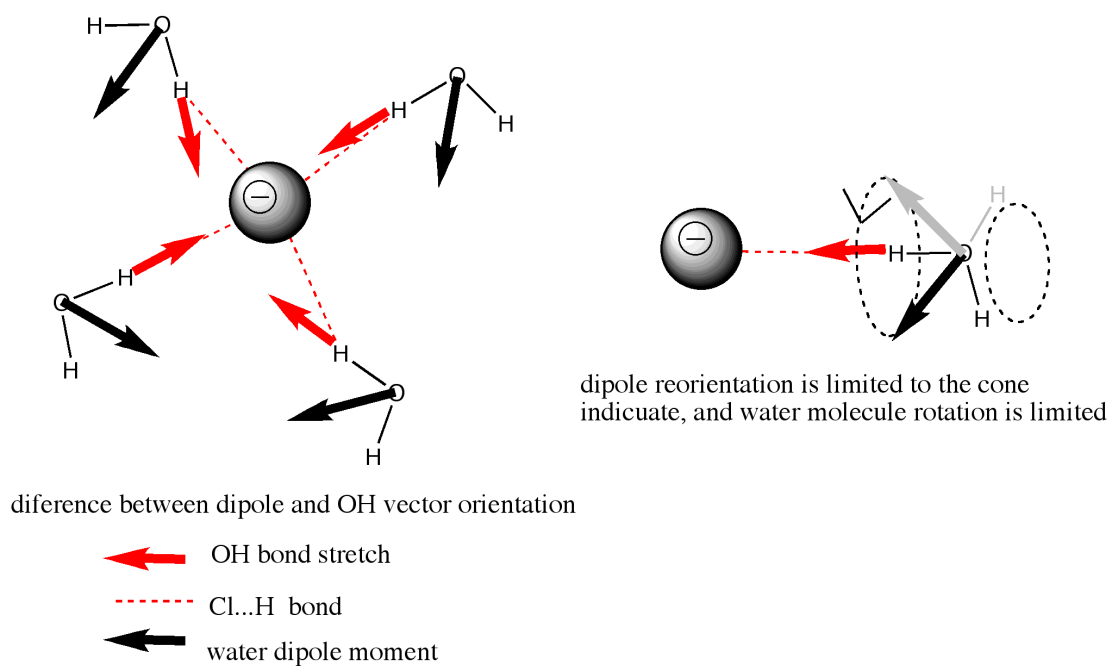


Figure S13: Cartoon showing the free reorientation of water dipole moment for a coordinated water molecule.

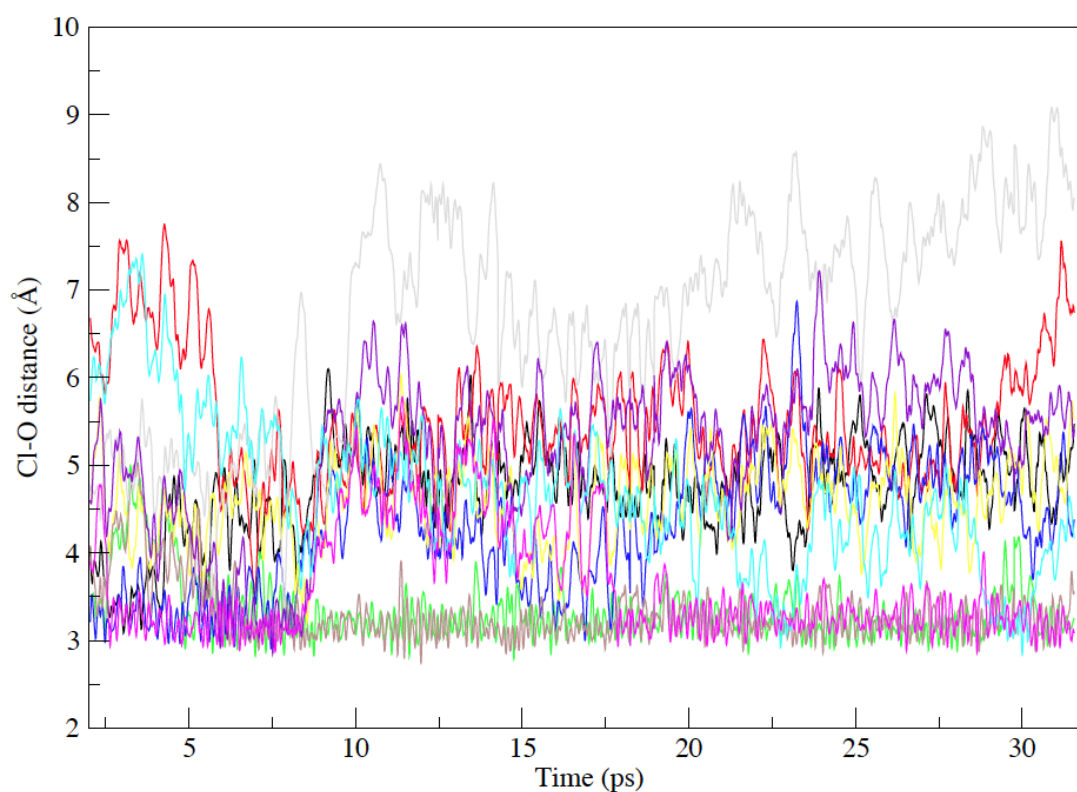


Figure S14: Time evolution of Cl-O distances along the CPMD simulation (31.56 ps; extended simulation) of aqueous chloride ($63\text{H}_2\text{O}+\text{Cl}^-$). Each line represents a water molecule. Only distances corresponding to the water molecules that belong to the first solvation shell at any time along the simulation are displayed.

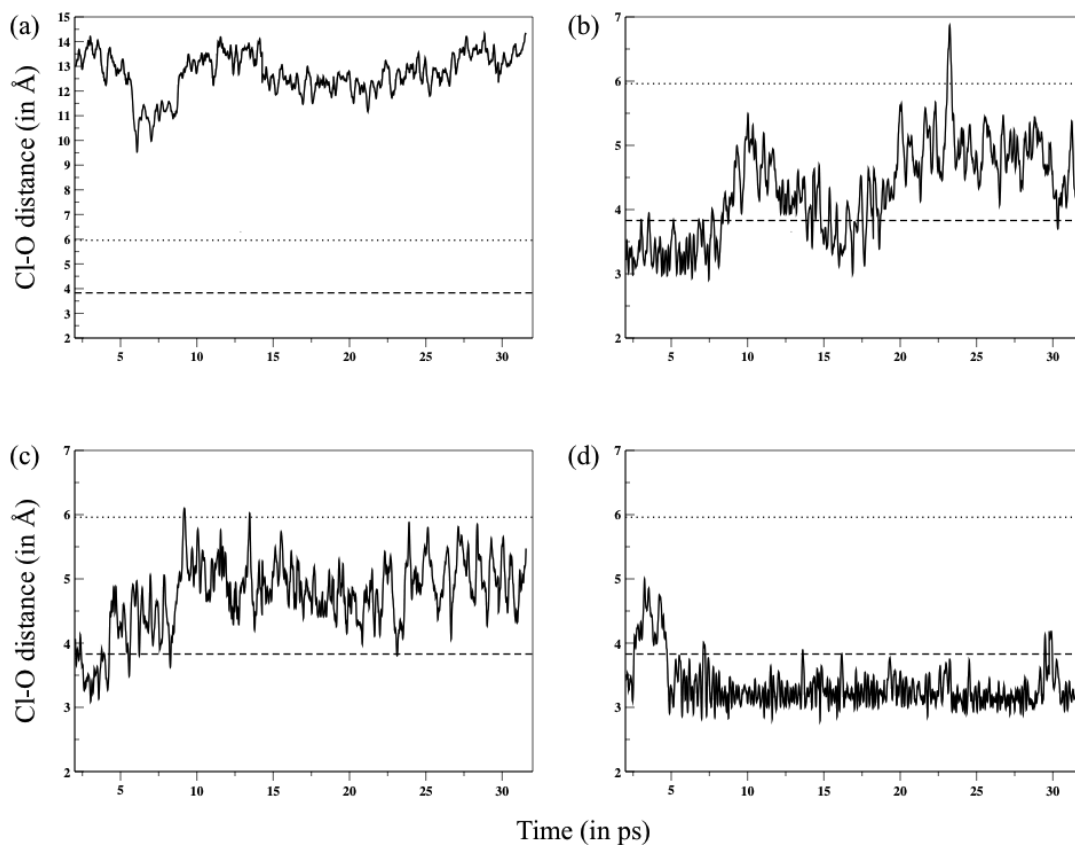


Figure S15 Time evolution of Cl-O distances along the Car-Parrinello simulation (31.56 ps; extended simulation) of aqueous chloride ($63\text{H}_2\text{O}+\text{Cl}^-$). The dashed line represents the first solvation shell radius (first minimum of the Cl-O RDF), and the dotted line represents the second solvation shell distance (second minimum of the Cl-O RDF). (a) representing water molecules always in bulk, (b) representing category (i), (c) representing category (ii), and (d) representing category (iii).

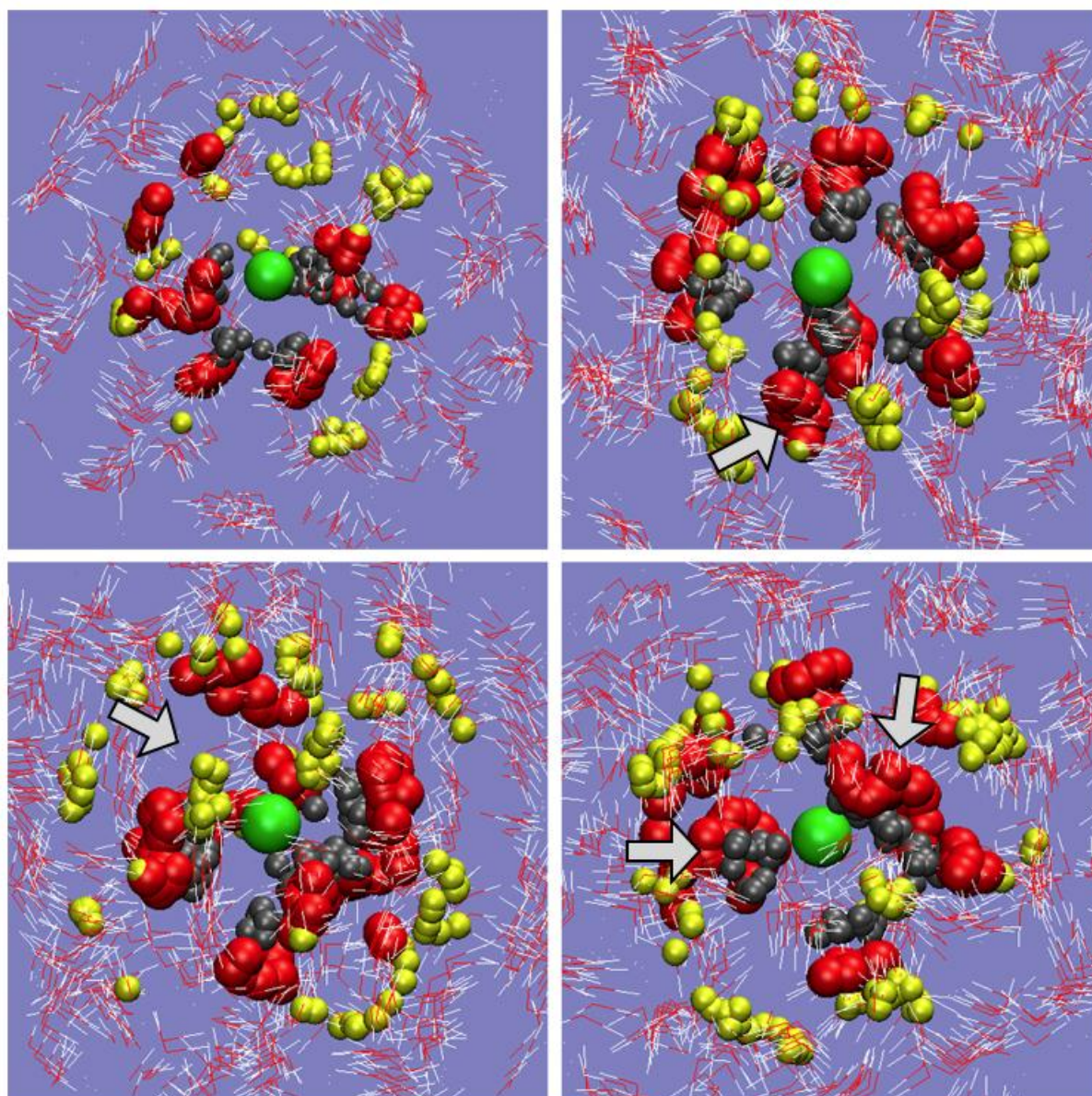


Figure S16: Time evolution around the Cl anion. H atoms within the Cl-H cut-off are grey, O atoms within the Cl-O cut-off are red, O atoms between 5.00 Å and the Cl-O cut-off are yellow, other water molecules as "lines". (a) shows the start of the segment, (b) shows the full segment (sampled from 600 steps), the arrow indicates a water molecule that has moved from outside the Cl-O boundary to within it, and also started to H-bond with the Cl. (c) shows the polar nature of the first solvation shell with the H-bonding water molecules collected on one side, and the "local" water molecules on the other side at a longer distance but still within the Cl-O cut-off. (d) shows the movement of H-bonded water molecules, more localised and focused than that of the "local" water molecules.